33RD CONGRESS
OF THE INTERNATIONAL COUNCIL
OF THE AERONAUTICAL SCIENCES
STOCKHOLM, SWEDEN, 4-9 SEPTEMBER, 2022

ICAS 2022 SWEDEN

CLUSTER STRUCTURE AND GATEWAY AVAILABILITY OF AD-HOC COMMUNICATION NETWORKS IN THE NORTH ATLANTIC AIRSPACE

Tobias Marks[1] & Alexander Hillebrecht[1]

[1]German Aerospace Center, Air Transportation Systems, Hamburg, Germany

Abstract

Data communication is an essential part of today's air traffic operations, enabling more flexible routing of aircraft and increased airspace capacity. While old generations of data link technology approach their technological limits, new technologies and approaches are being developed. Beside satellite communication and high frequency radio, one approach to enable data communication in remote, polar and oceanic airspaces such as the North Atlantic, is the establishment of aeronautical ad-hoc networks. Such networks are built up by direct data links between the aircraft which are acting as communication nodes, while ground connectivity is provided through dedicated gateway aircraft that are connected to ground. While the availability of gateways is strongly determined by the geographic location of the aircraft and ground stations, the connectivity of aeronautical ad-hoc networks is strongly influenced by the availability of gateways within clusters of inter-connected aircraft. In this paper, therefore, we follow an empirical approach to analyze the gateway availability and cluster structure on North Atlantic based on up to date flight plans. While an applicable set of ground stations is assumed that provides data transfer between ground and airborne network, we analyze the cluster structure and gateway availability by time-series analysis and present aggregated values for whole scenarios while varying the fraction of aircraft assumed to be equipped with the necessary technology as well as the air-to-air radio communication range. We show, that both factors have a strong influence on the formation of clusters and gateways and provide a starting point to derive requirements for the development of future communication technology.

Keywords: ad-hoc networks, communication, North Atlantic, air traffic

1. Introduction

The North Atlantic airspace is one of the busiest oceanic airspaces in the whole world (1), accommodating thousands of flights each day in both eastbound as well as westbound directions. However, as there is no radar coverage available, currently aircraft are widely separated on a timely basis, in order to maintain safety. Air traffic services (ATS) and airlines rely in terms of communication with aircraft on voice and data link communications via costly and high latency satellite links (2) or on the other hand via high frequency (HF) radio which is very limited in capacity while at the same time exhibiting high latencies as well. These limitations can lead to a reduced airspace capacity in the affected region (see e.g. (3)). In order to better handle the current air traffic load but also to accommodate a future air traffic growth in this region the capacity of the North Atlantic airspace needs to increase.
New data link technologies such as the L-band digital aeronautical communications system (LDACS) (see e.g. (4) and (5)) can help to achieve this goal by enhancing the communication between air traffic control (ATC) and aircraft, improving the situational awareness (3) as well as by enabling new data based applications such as self-separation or new en-route procedures like climate optimal routing ((6)) or aircraft wake-surfing for efficiency (AWSE) (see e.g. (7)) reducing the climate effect of aviation. Therefore, in the IntAirNet (Inter Aircraft Network) project that is funded by the German ministry of economic affairs and energy (BMWi) an air-to-air (A2A) data link based on the LDACS technology is being examined.

2. Related work

Compared to setting up direct data links to each individual aircraft, the creation of aeronautical ad-hoc networks (AANET) as proposed by (e.g. (8), (9) or (10)) using direct A2A data links represents a suitable method to enable communication among aircraft and between aircraft and ground in oceanic, remote and polar (ORP) airspaces without radio coverage. In order to establish air-to-ground (A2G) communication, the created AANETs need to be connected to ground based networks via dedicated network nodes acting as communication gateways. At these gateways the data volume is, therefore, drastically increased as all the traffic between the aircraft within the connected AANET cluster and ground entities need to be routed over the available gateways.
Hence, the formation of communication clusters within the airborne network along with the availability of gateways within these clusters is strongly determining the total connectivity and resulting data rates at particular aircraft in a given scenario. Additionally, the A2A communication range as well as the fraction of aircraft equipped with the new communication technology massively influence the cluster structure and gateway availability of the AANETs.
Several works deal with te creation of AANETs such as (11), (12), (13) or (14) mainly dealing with the routing aspect of the network. (15) follows an analytical approach to asses link probability, node degree and network coverage. However, none of these follow a systematic empirical approach to assess the above mentioned dependencies based on real world flight plan data.
In our work we, therefore, assess the global characteristics of the arrangement of clusters and gateways within a scenario or within a cluster of interconnected aircraft and use it to assess the overall connectivity of a scenario. These characteristics may include among others the total cluster amount and mean cluster sizes together with the total number of gateways enabling an airborne communication cluster to transfer data to and from ground. In combination with the structure of clusters, the analysis of gateways per cluster can lead to an even more profound understanding of the total connectivity of a scenario.

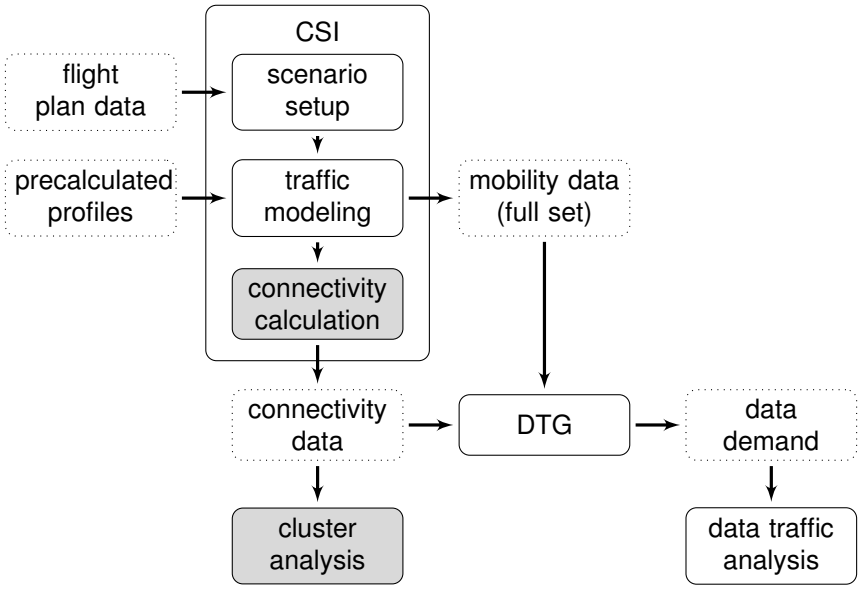

Figure 1 – General approach as followed within this work.

3. Methodology

Based on our air traffic connectivity modeling approach presented in a previous study (16) and our data communication demand model as presented in (17), in this paper we identify clusters of aircraft as well as such aircraft suitable to act as gateways for each timestamp given in a specific air traffic scenario.

3.1 General approach

The identification of clusters and gateways is a sub-process of the KOSMO connectivity simulator (CSI) as presented in (16). Figure 1 shows the general flowchart of the KOSMO tool. In KOSMO for a distinct flight plan the NAT air traffic is modeled using pre-calculated trajectory data. Based on this mobility dataset a connectivity calculation is performed identifying A2A and A2G connections for each specific timestamp. Within this connectivity calculation applicable algorithms identify coherent clusters of aircraft as well as gateways according to the cluster and gateway definitions given in section 3.4 The cluster and gateway data is appended to the basic connectivity data and handed over one the one hand to the KOSMO data traffic generator (DTG) that uses a data-traffic model (17) to calculate cluster based data traffic demand coverage as well as data rates. On the other hand the cluster data is aggregated and analyzed in terms of cluster sizes and gateway availability as it will be presented in this work.

3.2 Applicable simulation area

In order to focus on flights within the oceanic areas on North Atlantic, the applicable simulation area (ASA) is defined by the oceanic control area (OCA) boundaries on North Atlantic and while being limite southwards by 39th parallel. The respective OCAs are Gander (CZQX), Shanwick (EGGX), Bodo (ENOB), Reykjavik (BIRD), New York (KZWY) and Santa Maria (LPPO). Additionally, in order to cope for possible gateways close to the ASA border, a boundary region of 420km at the eastern and western ASA border was introduced. A detailed description of the ASA can be found in (16).

3.3 Air traffic modeling

For the modeling of air traffic flight plan data from first of August 2019 was used. As air traffic on the North Atlantic is forming two major traffic waves over the day, the data were filtered to contain only westbound flights. The applicable flights were then modeled by geodesics while pre calculated data from a trajectory calculation tool was used to provide realistic vertical flight profiles. For a more detailed description of the modeling of air traffic see (16).

3.4 Clusters and gateways

We define a cluster in our work as a set of interconnected aircraft within the ASA. The smallest possible cluster is, therefore, a set of two aircraft. A cluster is not required to have a gateway, however, a gateway inside a cluster is counted as a cluster node. If a gateway as part of a cluster is situated within the ASA boundary it is still counted as cluster node.

We define a gateway in this context as an aircraft that is connected to at least one ground station via an A2G data link while at the same time being connected by an A2A data link to at least one other aircraft, that is situated within the ASA and that is not having a ground connection by itself. We assume a A2G radio communication range r_g of 370km throughout this work. A set of 47 ground stations was assumed to provide data communication between the airborne and ground based networks. For more information on the selection of ground stations refer to (16).

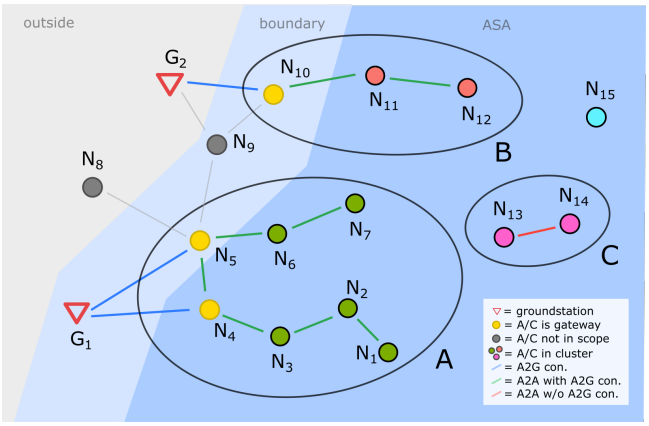

Figure 2 – Exemplary cluster situation at the edge of the ASA

Figure 2 shows schematically a typical situation of aircraft close to the border of the ASA. It can be seen, that nodes N_1... N_7 form cluster A, independent of the fact, that N_5 is outside the ASA as it is within the boundary. N_4 and N_5 act as gateways for cluster A, being connected to ground station G_1. N_8 is outside the scope of evaluation, whereas N_9 is not considered a gateway as it is not connected to an aircraft without ground connection in the ASA. N_{10}...N_{12} form cluster B with N_{10} acting as gateway being connected to ground station G_2. N_{13} and N_{14} form cluster C which is not connected to ground while N_{15} is considered an isolated flight not connected to a cluster and without ground connectivity.

3.5 Sets of aircraft

The amount of aircraft $\varphi(t)$ within the ASA at the particular timestamp t is given as the cardinality of the set of all aircraft $S(t)$ that are situated within the ASA at timestamp t according to

$$\varphi(t) = |S(t)| \tag{1}$$

The amount of all aircraft flying in clusters $\varphi_{cl}(t)$ or acting as a gateway $\varphi_{gw}(t)$ at timestamp t can then be defined accordingly as

$$\varphi_{cl}(t) = |S_{cl}(t)| \qquad \varphi_{gw}(t) = |S_{gw}(t)| \tag{2}$$

It needs to be mentioned, that as a gateway is not required to be situated in the ASA, the union of $S(t)$ and $S_{gw}(t)$ can be larger than $S(t)$ itself. Therefore, the results can be biased when comparing $\varphi_{cl}(t)$ or $\varphi_{gw}(t)$ with $\varphi(t)$. Hence, the comparison is made relative to the union $\varphi'(t)$ which is defined as

$$\varphi'(t) = |S(t) \cup S_{gw}(t)| \tag{3}$$

The size of individual clusters $\varphi_{cl,i}(t)$ is defined as the cardinality of the set of aircraft $S_{cl,i}(t)$ constituting cluster i at time t according to

$$\varphi_{cl,i}(t) = |S_{cl,i}(t)| \tag{4}$$

The average cluster size $\bar{\varphi}(t)$ across all clusters at a timestamp t in the particular scenario can then be calculated according to

$$\bar{\varphi}_{cl}(t) = \frac{1}{n_{cl}(t)} \sum_i \varphi_{cl,i}(t) \tag{5}$$

The number of gateways $\varphi_{gw,i}(t)$ within cluster i at timestamp t is defined as the cardinality of the intersection of the set of aircraft in the particular cluster and the set of gateway aircraft according to

$$\varphi_{gw,i}(t) = |S_{gw,i}(t)| = |S_{cl,i}(t) \cap S_{gw}(t)| \tag{6}$$

3.6 Basic metrics

Based on the calculation data we define the absolute number of clusters $n_{cl}(t)$ at a given timestamp t as the number of individual clusters according to the cluster definition. The absolute number of gateways at a given timestamp t is equal to $\varphi_{gw}(t)$. Beside the absolute numbers we define the number of clusters or gateways ($\psi_{cl}(t)$, $\psi_{gw}(t)$) relative to the amount of aircraft $\varphi'(t)$ at the particular timestamp as

$$\psi_{cl}(t) = \frac{n_{cl}(t)}{\varphi'(t)} \qquad \psi_{gw}(t) = \frac{\varphi_{gw}(t)}{\varphi'(t)} \tag{7}$$

According to the definition of a cluster the maximum value for $\psi_{cl}(t)$ cannot exceed $\frac{1}{2}$ meaning, that one cluster is formed for each pair of aircraft.

3.7 Gateways-per-clusters

Additionally we define a gateways-per-cluster metric $GPC(t)$ for a scenario at a distinct timestamp t by the fraction of the amount of aircraft acting as gateway and the amount of clusters.

$$GPC(t) = \frac{\varphi_{gw}(t)}{n_{cl}(t)} \tag{8}$$

3.8 Gateways-per-nodes

In order to cope with the gateway assignment to the single clusters in relation to the individual cluster sizes we additionally define the gateways-per-nodes metric $GPN_i(t)$ of cluster i at a given timestamp t as

$$GPN_i(t) = \frac{\varphi_{gw,i}(t)}{\varphi_{cl,i}(t)} \tag{9}$$

The average GPN across all clusters at a timestamp t in the particular scenario can then be calculated by averaging the individual GPN values across the clusters according to

$$GPN(t) = \frac{1}{n_{cl}(t)} \sum_i GPN_i(t) \tag{10}$$

Furthermore, in order to better account for the estimation of data rates within clusters an adapted GPN value is introduced as

$$GPN'(t) = \frac{1}{n_{cl}(t)} \sum_i GPN_i(t) \; \forall \; \{i \,|\, \varphi_{gw,i}(t) > 0\} \tag{11}$$

including only the clusters that exhibit at least one gateway.

3.9 Scenario metrics

In order to compare different scenarios on an aggregated level, we define the amount of clusters cumulated over all timestamps as well as the amount of aircraft acting as gateways cumulated over all timestamps per scenario as

$$N_{cl} = \sum_t n_{cl}(t) \qquad N_{gw} = \sum_t \varphi_{gw}(t) \tag{12}$$

In relation to the cumulated flight time of all applicable aircraft τ' as given by

$$\tau' = \sum_t \varphi'(t) \tag{13}$$

this results in the scenario metrics total relative amounts of gateways and clusters

$$\Psi_{cl} = \frac{N_{cl}}{\tau'} \qquad \Psi_{gw} = \frac{N_{gw}}{\tau'} \tag{14}$$

The gateways-per-cluster metric GPC for a whole scenario exhibiting n_t timestamps is given by averaging $GPC(t)$ over time according to

$$GPC = \frac{1}{n_t} \sum_t GPC(t) \tag{15}$$

For a whole scenario the gateways-per-node metrics $GPN(t)$ and $GPN'(t)$ can equally be averaged over time resulting in a total GPN and GPN' according to

$$GPN = \frac{1}{n_t} \sum_t GPN(t) \qquad GPN' = \frac{1}{n_t} \sum_t GPN'(t) \tag{16}$$

3.10 Communication range r_a and equipage fraction e_f

In order to understand the influence of the maximum A2A radio communication range (r_a) and the fraction of aircraft equipped with the new technology (equipage fraction, e_f) on the previously defined metrics, in our work we calculate a full set of variations of both parameters as defined in our previous study (16). Here, the r_a variation ranges form 0 to 420km in 15km steps whereas e_f is varied from 0 to 1 in 0.1 steps. To account for variations due to the random selection process of aircraft that is used to realize the particular equipage fraction if $e_f < 1$, we calculate 10 random samples for all parameter combinations which are consistent throughout the simulation for all variations of r_a.

4. Results

Based on the calculation data, in this section two major analyses will be presented. First, for a set of three selected example scenarios a time series analysis will be presented showing the development of clusters and gateways over time. Second, an aggregated analysis on scenario level will present the dependency of the cluster and gateway availability on communication range and equipage fraction.

4.1 Time series analysis

In this section the time series analyses for three different scenarios (A, B and C) with varying r_a and e_f as defined in (16) is presented. Table 1 reproduces the settings from this study. For all settings the first sample was used for the creation of plots.

Table 1 – Settings for example scenarios

parameter	setting A	setting B	setting C
direction	west	west	west
e_f	0.8	0.8	0.4
r_a	330 km	150 km	330 km

4.1.1 Cluster fractions

In order to get an understanding on how the aircraft are structured into clusters, figure 3 shows stacked plots of all aircraft within clusters over the simulation time t where each cluster of size $\varphi_{cl,i}(t)$ is represented by a different color. It has to be noted, that in this graph clusters are ordered and colored by size as individual clusters are not identified and traced over time.

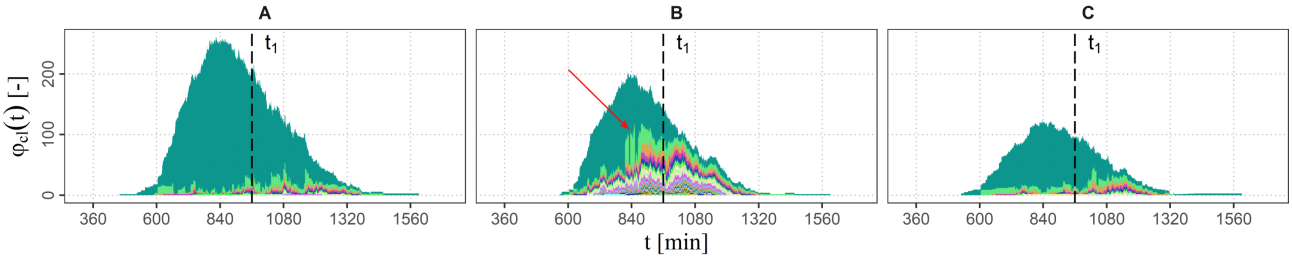

Figure 3 – Stacked plot of cluster sizes $\varphi_{cl,i}(t)$ for all example scenarios and over simulation time t

It can clearly be seen from the graphs, that with the tree example scenarios the distribution of aircraft to clusters strongly varies. Peaks in the data (as marked in scenario B) indicate the breaking up of bigger clusters into smaller ones. While in scenario A one large cluster can be identified over the span of simulation time in scenario B considerably more smaller clusters are formed due to the reduced r_a. At the same time in scenario B less aircraft are building up clusters in total, indicating that more isolated aircraft exist. In scenario C even less aircraft are constituting clusters due to the reduced e_f, however as in scenario A one large cluster can be identified over the span of simulation time.

The difference in cluster and gateway structure between the scenarios is getting more obvious while looking at the timestamp $t_1 = 960$. Figure 4 shows the situation of scenarios A and B at this particular timestamp. While in scenario A one large communication cluster of interconnected aircraft is formed

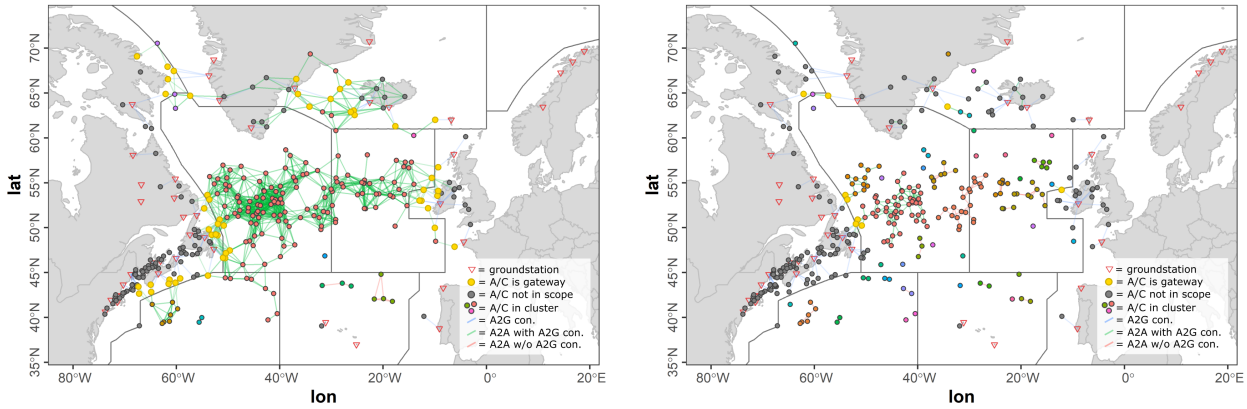

Figure 4 – Cluster and gateway situation at timestamp $t_1 = 960$ for scenario A (left) and B (right)

spanning the whole North Atlantic airspace in scenario B as a result of the reduced r_a this bridge is split into several smaller clusters that are not connected to ground. The reduced r_a additionally leads to a reduced number of gateways (shown in yellow).

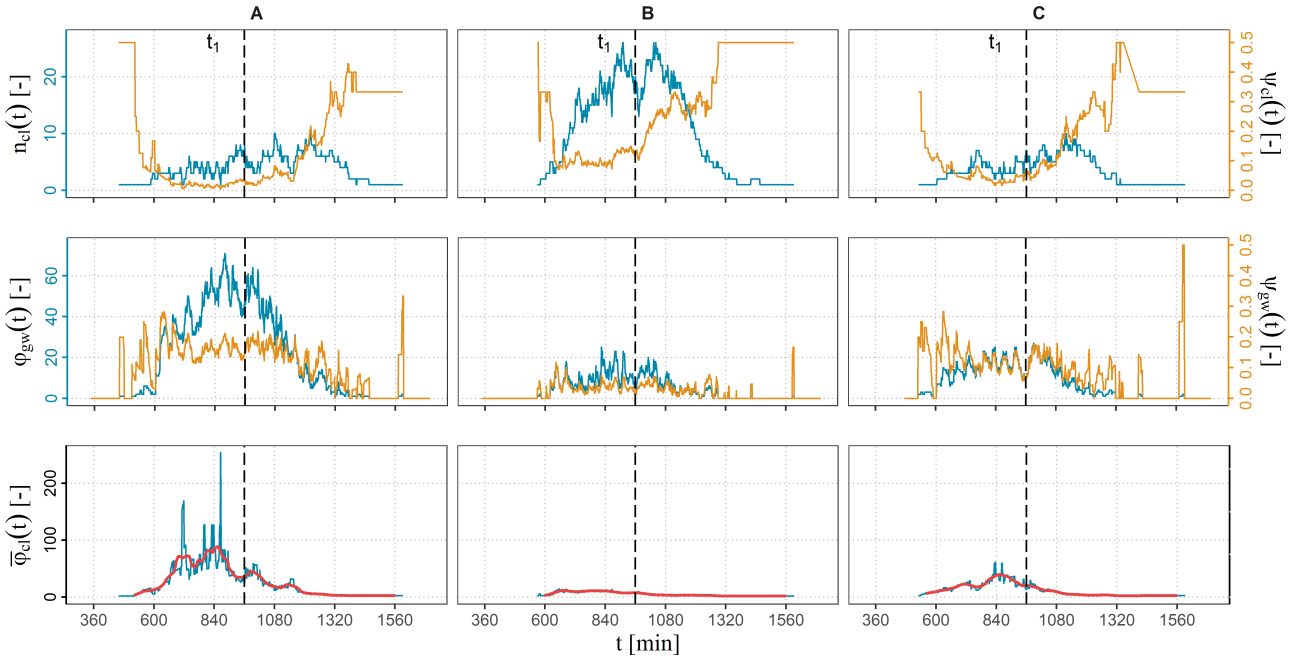

Figure 5 – Absolute ($n_{cl}(t)$) and relative ($\psi_{cl}(t)$) number of clusters (first row); absolute ($\varphi_{gw}(t)$) and relative ($\psi_{gw}(t)$) number of gateways (second row); average cluster sizes $\bar{\varphi}_{cl}(t)$ (third row); for all three example scenarios over the simulation time t

4.1.2 Number of clusters and gateways

Figure 5 shows the results for all three example scenarios showing the absolute ($n_{cl}(t)$) and relative ($\psi_{cl}(t)$) amount of clusters (first row) as well as the absolute ($\varphi_{gw}(t)$) and relative ($\psi_{gw}(t)$) amount of gateways (second row) over the simulation time t. As the amount of aircraft within the ASA is almost normally distributed over t (see (16)), in scenario B the highest values for $n_{cl}(t)$ occur roughly following the distribution of aircraft density. For scenarios A and C it can be observed, that the values for $n_{cl}(t)$ seem to be more independent of the aircraft density while the relative amount of clusters $\psi_{cl}(t)$ is getting close to 0 during the peak hours, meaning the aircraft in the ASA can be associated to a small number of big clusters. During the beginning and at the end of the period, when only a few airplanes are located within the ASA, $\psi_{cl}(t)$ is reaching values of about 0.5 meaning each pair of aircraft constitutes an individual cluster.

For the gateways it can be observed, that $\varphi_{gw}(t)$ basically follows the distribution of the aircraft density while higher communication ranges (A and C) result in more available gateways. This can be expected, as the more aircraft are located within the ASA and the ASA boundary the more can act as gateways. $\psi_{gw}(t)$ is showing a very variable distribution over the simulation time while reaching 0.5 at the start and the beginning. Scenarios A and C show similar values for $\psi_{gw}(t)$ while the values in scenario B are considerably smaller.

4.1.3 Average cluster sizes

Figure 5 (third row) shows the results for the average cluster sizes $\bar{\varphi}_{cl}(t)$ over simulation time t. The curves for the moving averages of order 60 are superimposed in red. From the data it can be observed that in scenario A the average cluster size increases during the times with high traffic reaching values of more than 100 nodes per cluster. Furthermore, several distinct peaks can be observed in the data indicating the breaking up of large clusters into smaller ones. In scenario B as expected due to the reduced A2A communication range r_a considerable smaller clusters are formed while in scenario C the average cluster size resides in between the values from scenarios A and B while reaching the highest values during the peak traffic times.

4.1.4 GPC(t), GPN(t) and GPN'(t)

Figure 6 shows the $GPC(t)$ (first row), $GPN(t)$ (second row) as well as $GPN'(t)$ (third row) for all three scenarios over the simulation time t. The curves for the moving averages of order 60 are superimposed in red.

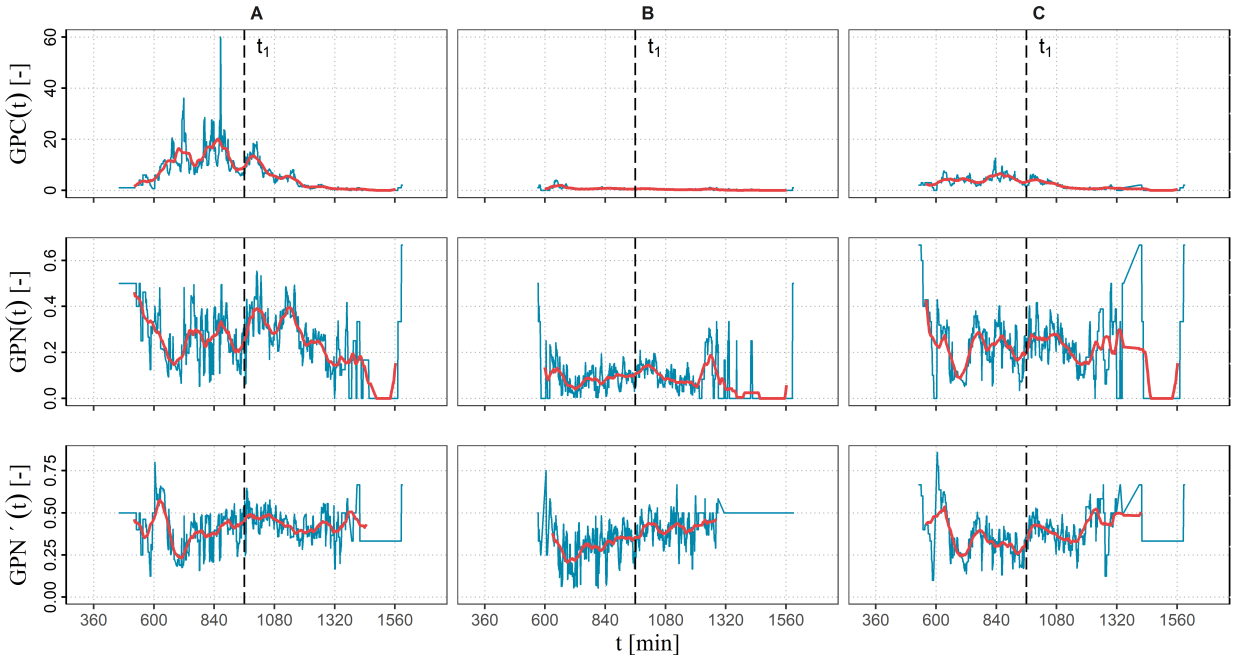

Figure 6 – $GPC(t)$ (first row), $GPN(t)$ (second row) and $GPN'(t)$ (third row) for all tree example scenarios over simulation time t; moving averages of order 60 are superimposed in red

It can be observed from the data, that while the GPC values roughly follow the distribution of the aircraft density the $GPN(t)$ and $GPN'(t)$ values distribute more independently. The $GPC(t)$ show a clear dependency on both r_a and e_f with scenario A reaching values of up to 60 while in scenario B the values remain most of the time below 5. In contrast to this, the average $GPN(t)$ values same as the values for $\psi_{gw}(t)$ are strongly varying with time showing values in the range of 0 to 0.6. In scenarios A and C the $GPN(t)$ values reach comparable levels, while in scenario B $GPN(t)$ is residing most of the time below 0.2. For $GPN'(t)$ representing clusters with gateways only this in not the case. Here all scenarios reach comparable values.

4.2 Influence of r_a and e_f

In a next step of our analysis the metrics will be compared on scenario level for the whole set of parameter variations of r_a and e_f as defined in section 3.10 In the plots not showing a contour, the means across the samples are marked by a solid line while the 95% confidence intervals are shown as shaded areas additionally. For further interpretation of the results in all plots the tree example scenarios are marked in red.

4.2.1 Total relative amount of clusters and gateways

Figure 7 shows the results for Ψ_{cl} (left) and Ψ_{gw} (right) depending on r_a and e_f. It can be observed, that the values for Ψ_{cl} show a steep increase with r_a while reaching a maximum value after which the curves decrease again. The higher e_f the earlier this maximum is reached. This can be explained by the fact that with low communication ranges only a few clusters are forming. With increasing r_a the clusters grow until a maximum of independent clusters is reached. A further increase of r_a will result in a merging of the smaller clusters into bigger ones reducing the cluster amount. The more aircraft are within the scenario the earlier this consolidation effect seems to occur. However, it can be expected that with a further increase of r_a a saturation will occur when all aircraft are ultimately forming one big cluster. Furthermore, the higher e_f the less the curves are influenced while lower e_f show a higher variability of data as can be expected due to the increased variability in selecting the subset of aircraft.

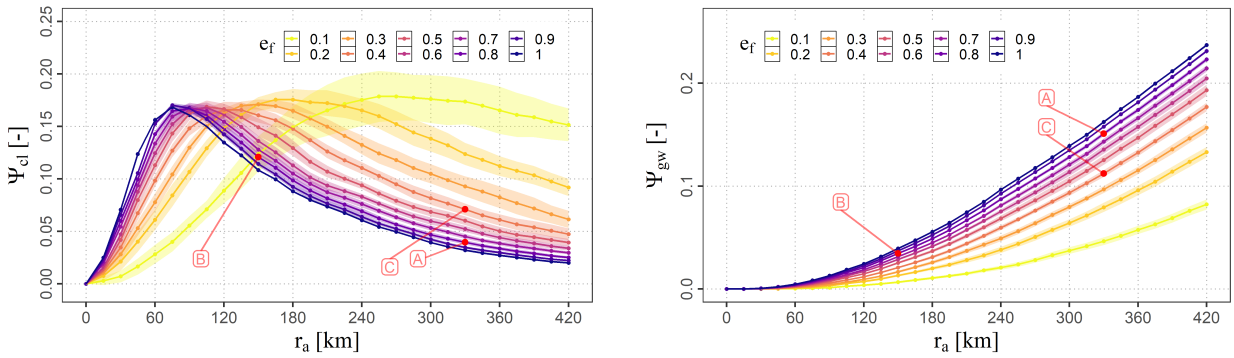

Figure 7 – Total relative amount of clusters Ψ_{cl} (left) and gateways Ψ_{gw} (right) cumulated over time for variations of r_a and e_f

The curves for Ψ_{gw} show an initial exponential increase of the values flattening to an almost linear trend for increasing r_a. The higher e_f the less the curves are influenced while the variability of data resides in a comparable range for the different equipage fractions. This seems reasonable, as the higher the communication range and the more aircraft are in the scenario, the more aircraft can act as gateways and connect the clusters to ground. However, it can be expected that with a further increase of r_a again a saturation will occur when all aircraft meeting the requirements of being a gateway are also acting as such.

4.2.2 Total GPC

Figure 8 (left) shows the results for the total GPC depending on r_a and e_f. From the data it can be observed, that the values for GPC increase exponentially by r_a and e_f. This can be expected, as the bigger the clusters become the less clusters exist in the scenario while at the same time more gateways become available. However, it can be expected that same as for Ψ_{gw} a saturation will occur if r_a further increases up to a point when all aircraft form only one cluster and all applicable gateways connect this single cluster to ground. Furthermore, it needs to be mentioned, that the variability of data is highest for $0.4 < e_f < 0.6$ as it can be seen from size of the confidence intervals in figure 8.
Figure 8 (right) additionally shows the results for the means across the samples of the total GPC depending on r_a and e_f as a contour plot. From the plot it can be seen, that the influence of r_a on total GPC is stronger than of e_f. The mean total GPC values for a combination of r_a and e_f can be easily extracted from the plot.

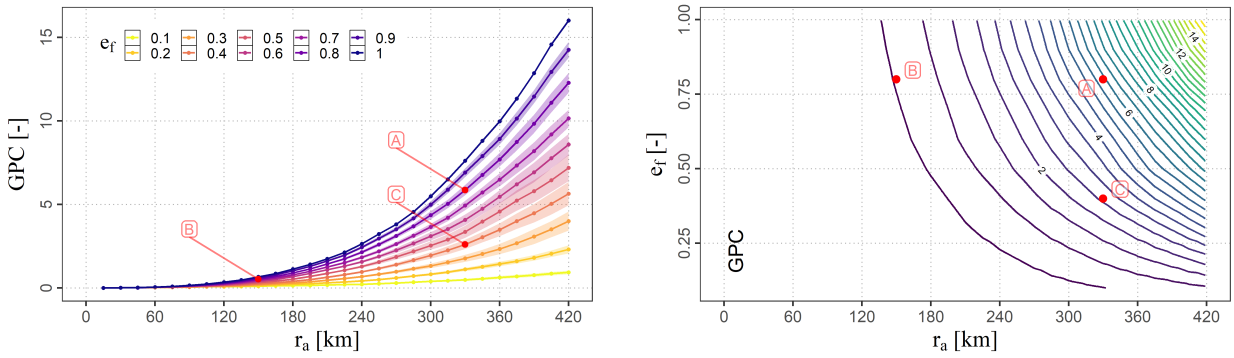

Figure 8 – Total GPC (left) and contour plot of mean values (right) for variations of r_a and e_f

4.2.3 Total GPN and GPN'

Figure 9 (left) shows the results for the total GPN depending on r_a and e_f. It can be observed, that in contrast to the total GPC the total GPN values seem show with increasing r_a after a first exponential increase a linear or for higher values of e_f even a negative trend. Maximum values of $GPN > 0.3$ are reached. Furthermore, it can be observed, that for high values of r_a the total GPN is not further increasing with e_f. The variability of the data seems to be comparable for the different equipage fractions. Figure 9 (right) additionally shows the results for the means across the samples of the total GPN depending on r_a and e_f as a contour plot. The results indicate, that especially for higher values of r_a values of $e_f > 0.5$ are not leading to a higher availability of gateways per nodes.

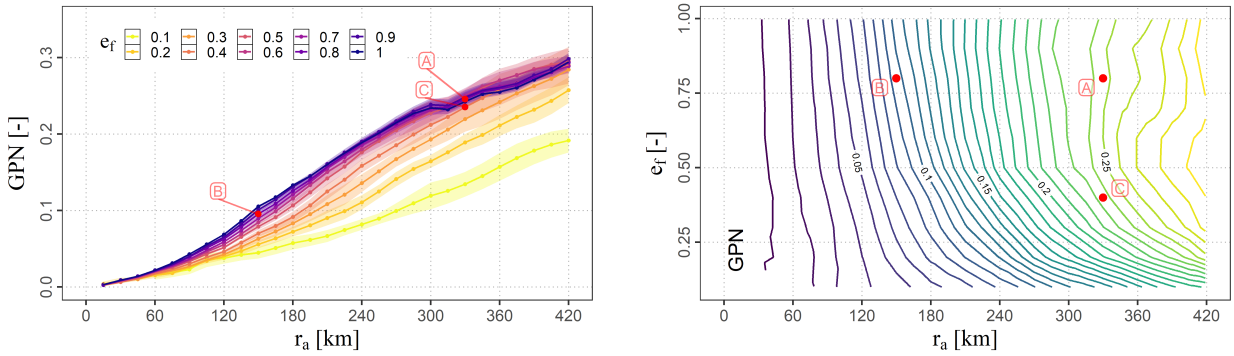

Figure 9 – Total GPN (left) and contour plot of mean values (right) for variations of r_a and e_f

Figure 10 (left) shows the results for the total GPN' depending on r_a and e_f. From the data it can be observed, that the values for GPN' generally are in the range of $0.35 < GPN' < 0.5$ and decrease by increasing r_a until reaching a minimum. Similar to Ψ_{cl} the higher e_f this minimum is reached at lower values of r_a. A further increase of r_a results in an increase in total GPN'. This effect can be attributed to the consolidation of clusters already mentioned above.

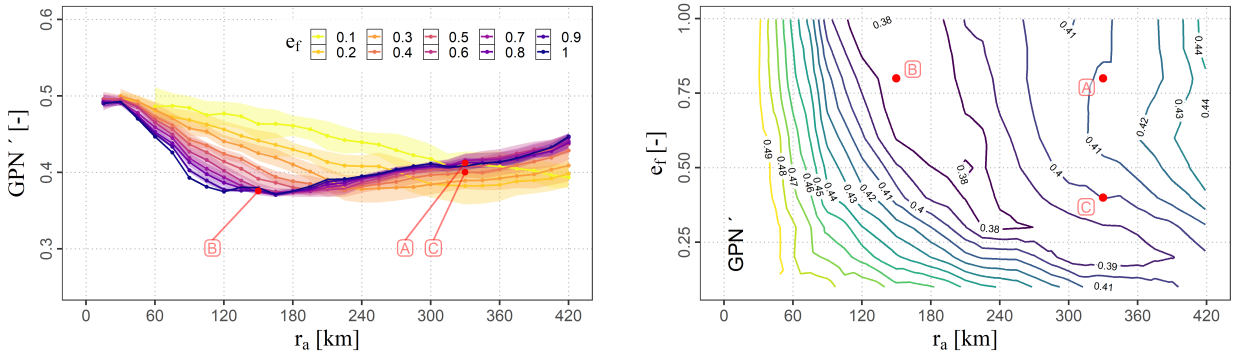

Figure 10 – Total GPN' (left) and contour plot of mean values (right) for variations of r_a and e_f

Figure 10 (right) additionally shows the results for the means across the samples of the total GPN' depending on r_a and e_f as a contour plot. It can be seen, that the dip showing low values reaches from low e_f and high r_a to high values of e_f and r_a of about 150km.
As the total GPN' has a significant influence on data rates at the gateway aircraft it seems reasonable to avoid this dip when deriving requirements fur future communication technologies. In combination with the total GPN that includes clusters not connected to ground, both GPN and GPN' should be maximized. Therefore, the range of $r_a > 240km$ and $e_f > 0.5$ can be assumed to be favorable in order to maximize connectivity in AANETs. However, due to the empirical character of the study and the limited samples assessed, additional research is needed to assure this assumption.

5. Discussion and outlook

In this paper we introduced a methodology to assess gateways and clusters within aeronautical ad-hoc communication networks in the North Atlantic airspace using the air traffic modeling approach presented by the authors in a previous work (16). Based on this methodology we assessed the strong dependency of cluster and gateway availability in such networks on A2A communication range, equipage fraction and time. We showed by time series analysis, that the amount of clusters and average cluster size as well as the amount of available gateways is highly dynamic over time depending on the aircraft density in the applicable region and the assumed communication range. Peaks in the cluster distribution indicate, that bigger clusters frequently break up into smaller ones. Large clusters over large parts of simulation time appear only if the communication range is sufficiently high. Furthermore, we showed, that the amount of available gateways in relation to the amount of clusters basically follows the density of available aircraft while the gateways within each cluster in relation to the nodes constituting the particular cluster in average are more independent of the available aircraft in the scenario.

As compared on scenario level the results suggest, that A2A communication range has a stronger influence on cluster size than equipage fraction. The available gateways in relation to the number of clusters are rising exponentially, as the bigger the clusters get the less individual clusters are formed while at the same time more gateways become available in the scenario. The analysis of available gateways per nodes on cluster level shows, that the values are not as dependent on equipage fraction than on A2A communication range. The results indicate, that especially for higher A2A communication ranges an equipage fraction of more than 50% will not lead to higher availability of gateways per nodes. When considering only clusters exhibiting at least one gateway, the data shows a dip with reduced gateway availability. To avoid this dip, the range of an A2A communication range of more than 240km and an equipage fraction of more than 50% seems reasonable to assume when deriving requirements for future communication technologies. Relations of gateways to cluster nodes > 0.4 can be reached. However, further investigation is needed to confirm this finding.

While looking at real world data communication, not only the availability of gateways is limiting the communication in aeronautical ad-hoc networks also the occurrence of bottlenecks within the clusters can lead to reduced connectivity and high data rates at the particular aircraft. In order to derive requirements for future communication technologies an assessment of these bottlenecks is necessary. Furthermore in our studies we only investigated the westbound traffic on North Atlantic. A similar investigation for eastbound traffic as well as for other traffic scenarios seems to be worthwhile especially when looking at the post-COVID air traffic situation. In this context its needs to be mentioned, that a bigger part of North Atlantic air traffic is routed over the organized track system (OTS). The thereby invoked channeling of aircraft on the particular OTS tracks will influence the connectivity of aircraft. Same is true for the daily adaption of the tracks due to the prevalent wind and traffic situation. The modeling of air traffic using the OTS or the connectivity analysis based on real world flight tracks will help to assess these effects in the future.

Funding

The work presented in this paper was part of the project IntAirNet that was funded by the German Ministry of Economic Affairs and Energy (BMWi) under the National Aeronautical Research Program

(LuFo) V-3 under the grant agreement no. 20V1708B.

Contact Author Email Address

tobias.marks@dlr.de

Copyright Statement

References

[1] EUROCONTROL, "Five-Year Forecast 2020-2024," tech. rep., EUROCONTROL, 11 2020. STATFOR Ref. DOC677.

[2] ICAO, *NORTH ATLANTIC OPERATIONS AND AIRSPACE MANUAL*. International Civil Aviation Organization, 2021. NAT Doc 007/V.2021-1.

[3] B. Welch and I. Greenfield, "Oceanic situational awareness over the north atlantic corridor," tech. rep., NASA Glenn Research Center, Cleveland, OH, United States, Feb. 2005.

[4] N. Neji, R. de Lacerda, A. Azoulay, T. Letertre, and O. Outtier, "Survey on the Future Aeronautical Communication System and Its Development for Continental Communications," *IEEE Transactions on Vehicular Technology*, vol. 62, no. 1, pp. 182–191, 2013.

[5] M. Schnell, U. Epple, D. Shutin, and N. Schneckenburger, "LDACS: Future Aeronautical Communications for Air-Traffic Management," *Communications Magazine, IEEE*, vol. 52, pp. 104–110, 05 2014.

[6] V. Grewe, K. Dahlmann, J. Flink, C. Frömming, R. Ghosh, K. Gierens, R. Heller, J. Hendricks, P. Jöckel, S. Kaufmann, K. Kölker, F. Linke, T. Luchkova, B. Lührs, J. Van Manen, S. Matthes, A. Minikin, M. Niklaß, M. Plohr, M. Righi, S. Rosanka, A. Schmitt, U. Schumann, I. Terekhov, S. Unterstrasser, M. Vázquez-Navarro, C. Voigt, K. Wicke, H. Yamashita, A. Zahn, and H. Ziereis, "Mitigating the climate impact from aviation: Achievements and results of the dlr wecare project," *Aerospace*, vol. 4, no. 3, 2017.

[7] D. Erbschloe, A. Antczak, D. Carter, G. Dale, C. Döll, R. Luckner, T. Marks, and M. Niestroy, "Operationalizing flight formations for aerodynamic benefits," vol. 1 PartF, 2020. cited By 3.

[8] D. Medina, F. Hoffmann, S. Ayaz, and C. Rokitansky, "Feasibility of an aeronautical mobile ad hoc network over the north atlantic corridor," *Proceedings of 5th Annual IEEE Communications Society Conference on Sensor, Mesh and Ad Hoc Communications and Networks*, pp. 109–116, 2008.

[9] T. Ho and S. Shigeru, "A Proposal of Relaying Data in Aeronautical Communication for Oceanic Flight Routes Employing Mobile Ad-Hoc Network," pp. 436–441, 04 2009.

[10] T. Ho and S. Shigeru, "Mobile ad-hoc network based relaying data system for oceanic flight routes in aeronautical communications," *International journal of Computer Networks Communications*, vol. 1, 04 2009.

[11] Q. Vey, A. Pirovano, J. Radzik, and F. Garcia, "Aeronautical Ad Hoc Network for Civil Aviation," *Communication Technologies for Vehicles*, pp. 81–93, 2014.

[12] E. Sakhaee, A. Jamalipour, and N. Kato, "Aeronautical ad hoc networks," *IEEE Wireless Communications and Networking Conference, 2006. WCNC 2006.*, vol. 1, pp. 246–251, 2006.

[13] D. Medina, F. Hoffmann, F. Rossetto, and C.-H. Rokitansky, “Routing in the Airborne Internet,” *Proceedings of 2010 Integrated Communications, Navigation, and Surveillance Conference*, pp. A7–1–A7–10, 2010.

[14] D. Medina, *Geographic Load Share Routing in the Airborne Internet*. PhD thesis, Paris Lodron Universität Salzburg, Juli 2011.

[15] L. F. M. Vieira, M. G. Almiron, and A. A. F. Loureiro, “3d manets: Link probability, node degree, network coverage and applications,” in *2011 IEEE Wireless Communications and Networking Conference*, pp. 2042–2047, 2011.

[16] T. Marks, A. Hillebrecht, and F. Linke, “Modeling air-to-air communication networks in the North Atlantic region,” *(under review), CEAS Aeronautical Journal, Springer International Publishing*, 2022.

[17] A. Hillebrecht, T. Marks, and V. Gollnick, “An Aeronautical Data Trafiic Model for the North Atlantic Oceanic Airspace,” *(under review), CEAS Aeronautical Journal, Springer International Publishing*, 2022.